International Journal of
Mathematics And its Applications
ISSN: 2347-1557

Int. J. Math. And Appl., **14(2)**(2026), 253–265
Available Online: http://ijmaa.in

Slip Velocity and Chemical Reaction Effects on Unsteady Free Convection Flow of MHD Casson Fluid in a Cylinder with Heat and Mass Transfer Through Porous Medium

Vinod Kumar[1,*], Gaurav Kumar[1]

[1]*Department of Mathematics and Computer Science, Babu Banarasi Das University, Lucknow, Uttar Pradesh, India*

Abstract

This research paper is focused on a study of the unsteady MHD flow of non-Newtonian Casson fluid with slip velocity and chemical reaction effect in the presence of heat and mass diffusion. The fluid flows past in infinite circular cylinders through a porous medium. The analytic solutions for the velocity profile are derived by using the Laplace transform and the finite Hankel transform. The graphical profiles of velocity are represented to examine and illustrate the impacts of various physical parameters on the significance of physical flow features. The result shows that the slip velocity in the presence of chemical reaction influenced the behaviour of the flow of Casson MHD fluid velocity. Besides that, fluid velocity increases with the increase in the Casson parameter, while it decreases when the magnetic parameter increases. The impact of slip velocity on the flow of fluid decreases at the centre and increases at the boundary of a cylinder. Thus, these findings are beneficial for further exploration in the applications of biomedical engineering and pathology.

Keywords: Casson fluid; Slip velocity; chemical reaction; porous medium.
2020 Mathematics Subject Classification: 76S05, 80Axx, 76D05.

1. Introduction

The significance of the Casson fluid flow model is used to characterize the non-Newtonian fluid behavior. The Casson MHD fluid model is based on rheological liquids, which are applicable in biotechnology, medical science, chemical engineering, etc. Therefore, many researchers investigate the behaviour of the Casson fluid flow through a porous medium in the cylindrical domain because it is more relevant to real-life applications such as pipeline flow, blood flow in a vessel, and others. The slip velocity is defined as the finite velocity of a fluid at a boundary or surrounded within an area (Nubar [1]). Combined heat and mass transfer in natural convection along a vertical cylinder was investigated by Chen and Yuh [2]. For example, in medical science applications, blood flow in an artery is under pathological situations when fatty plaques and blood clots are formed in the artery (Das et al. [3]).

*Corresponding author (vermavinod735@gmail.com)

Dash et al. [4] have worked on the Casson fluid flow in a pipe filled with a homogeneous porous medium. In the earliest studies, non-Newtonian flow in porous media was discussed by Sochi [5]. Nadeem et al. [6] have defined the solution of the MHD flow model based on a Casson fluid over an exponentially shrinking sheet. Khalid et al. [7] have worked on unsteady MHD free convection flow of Casson fluid past an oscillating vertical plate embedded in a porous medium. Animasaun et al. [8] have worked on Casson fluid flow with variable thermophysical properties by using the homotopy method. They have noticed that an increase in the variable plastic dynamic viscosity of Casson fluid corresponds to an increase in the flow velocity. Heat transfer analysis of boundary layer flow over a hyperbolic stretching cylinder was studied by Majeed et al. [9], and they obtained the numerical results for the model by a finite difference scheme.

Afify [10] has determined the solution of the flow model, assuming the influence of slip boundary conditions on Casson nanofluid flow over a stretching sheet in the presence of viscous dissipation and chemical reaction. Khan et al. [11] have discussed the analytic solution of natural convection heat transfer in an oscillating vertical cylinder. Azmi et al. [12] have obtained the analytical solution of unsteady Casson fluid flow. They obtained that an increase in curvature parameter leads to an increase in flow velocity with temperature distribution. They have also found that the skin-friction coefficient reduces and the Nusselt number enhances with an increase in curvature parameter. Studying the magnetic field in the porous medium is significant. The role of chemical reactions, along with heat and mass transfer, is fundamental in industrial applications such as food processing and polymer production. Kumar and Rizvi [13] have explored the impact of Casson fluid flow past a vertical cylinder in the presence of chemical reaction and magnetic field. Kumar et al. [14] have worked on unsteady MHD flow through a porous medium past an inclined cylinder in the presence of chemical reaction, and the MHD flow model is solved numerically by using the Crank-Nicolson method. The study of slip velocity at the boundary is significant for fluid velocity because it is influenced by the viscosity and behaviour of the fluid model. As fluid slips on the wall, effects are seen in many domains, including micro- and nano-channels. It is often used in applications where a very thin coating of oil is sprayed onto a moving surface of a vertical cylinder with a slip velocity effect. Further, Azmi et al. [15] studied the slip velocity effect on the unsteady free convection flow of Casson fluid in a vertical cylinder. They have used Laplace and Hankel transform techniques to solve the MHD flow model and analyzed the fluid velocity decreases with Casson and Prandtl number parameters. The flow model under assumptions, such as the impact of slip velocity and chemical reaction effects on unsteady free convection flow of MHD Casson fluid in a cylinder with heat and mass transfer. The problem of the flow model is solved analytically by using the Laplace and finite Hankel transforms method, and zeros of the Bessel functions were also used to obtain graphical results illustrating the various effects of parameters involved in the MHD fluid model.

2. Mathematical Modelling

The geometrical model of the problem is shown in Figure 1.

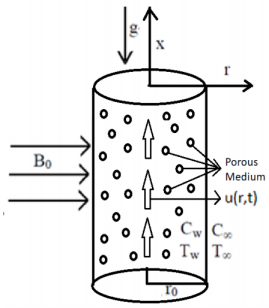

Figure 1: Physical model of the MHD flow.

In the present paper, we consider unsteady MHD chemically reacting and electrically conducting Casson fluid flow through a cylinder of radius r_0. Here, the x-axis is taken along the axis of the cylinder in the vertical direction, and the radial coordinate r is taken normal to the surface. The uniform strength magnetic field B_0 is applied perpendicular to the surface of the cylinder. Initially, it is assumed that the surface of the cylinder and the fluid are at the same temperature, T_∞. The species concentration in the fluid is considered as C_∞ for all $t = 0$. At time $t > 0$, the temperature of the surface T_w and the concentration C_w near the surface are raised. Then, under these assumptions, the MHD Casson fluid model is:

Equations of motion

$$\frac{\partial u}{\partial t} = v\left(1+\frac{1}{\gamma}\right)\frac{\partial^2 u}{\partial r^2} + \frac{v}{r}\left(1+\frac{1}{\gamma}\right)\frac{\partial u}{\partial r} + g\beta\,(T-T_\infty) + g\beta^*\,(C-C_\infty) - \frac{\sigma B_0^2 u}{\rho} - \frac{vu}{K} \tag{1}$$

Equation of energy

$$\frac{\partial T}{\partial t} = \alpha\frac{\partial^2 T}{\partial r^2} + \frac{\alpha}{r}\frac{\partial T}{\partial r} \tag{2}$$

Diffusion equation

$$\frac{\partial C}{\partial t} = D\frac{\partial^2 C}{\partial r^2} + \frac{D}{r}\frac{\partial C}{\partial r} - K_C(C-C_\infty) \tag{3}$$

Initial and boundary conditions are as follows:

$$\begin{aligned} &u(r,0) = 0, \quad T(r,0) = T_\infty, \quad C(r,0) = C_\infty, \quad r \in [0,r_0], \\ &u(r_0,t) = u_s, \quad T(r_0,t) = T_w, \quad C(r_0,t) = C_w; \quad t > 0 \\ &\tfrac{\partial u(0,t)}{\partial r} = 0, \quad \tfrac{\partial T(0,t)}{\partial r} = 0, \quad \tfrac{\partial C(0,t)}{\partial r} = 0; \quad t > 0 \end{aligned} \tag{4}$$

Here u is the velocity of fluid, g-the acceleration due to gravity, β-volumetric coefficient of thermal expansion, t-time, T-temperature of the fluid, β^*-volumetric coefficient of concentration expansion, C-species concentration in the fluid, ν-the kinematic viscosity, ρ-the density, C_p-the specific heat at constant pressure, k-thermal conductivity of the fluid, D-the mass diffusion coefficient, T_w-temperature

of the plate at $z = 0$, C_w-species concentration at the surface, B_0-the uniform magnetic field, K-the permeability parameter, σ- electrical conductivity.

The following dimensionless quantities are used to transform the above equations into non-dimensional form:

$$\begin{aligned} &R = \tfrac{r}{r_0}, \quad \bar{u} = \tfrac{u}{u_0}, \quad \bar{u}_s = \tfrac{u_s}{u_0}\theta = \tfrac{(T-T_\infty)}{(T_w-T_\infty)}, \quad S_c = \tfrac{v}{D}, \quad \mu = \rho v, \quad \bar{\omega} = \tfrac{\omega v}{u_0^2}, \quad P_r = \tfrac{v}{\alpha}, \\ &\bar{C} = \tfrac{(C-C_\infty)}{(C_w-C_\infty)}, \quad G_r = \tfrac{g\beta v(T_w-T_\infty)}{u_0^3}, \quad M = \tfrac{\sigma B_0^2 r_0^2}{v\rho}, \quad G_m = \tfrac{g\beta^* v(C_w-C_\infty)}{u_0^3}, \\ &\bar{b} = \tfrac{bv}{u_0^2}, \quad \gamma = \tfrac{\mu_B\sqrt{2\pi}}{p_y}, \quad \bar{K} = \tfrac{u_0}{v^2}K, \quad \bar{t} = \tfrac{tv}{r_0^2}. \end{aligned} \tag{5}$$

The symbols in dimensionless form are as follows:

$\bar{u}$ is the dimensionless Primary velocity, $\bar{v}$-the secondary velocity, $\bar{t}$-dimensionless time, θ-the dimensionless temperature, $\bar{C}$-the dimensionless concentration, G_r-thermal Grashof number, G_m-mass Grashof number, μ-the coefficient of viscosity, $\bar{K}$-the dimensionless permeability parameter, P_r-the Prandtl number, S_c-the Schmidt number, M-the magnetic parameter.

The dimensionless MHD model is:

$$\frac{\partial \bar{u}}{\partial \bar{t}} = \left(1+\frac{1}{\gamma}\right)\frac{\partial^2 \bar{u}}{\partial R^2} + \frac{1}{R}\left(1+\frac{1}{\gamma}\right)\frac{\partial \bar{u}}{\partial R} + G_r\theta + G_m\bar{C} - M\bar{u} - \frac{1}{\bar{K}}\bar{u} \tag{6}$$

$$\frac{\partial \theta}{\partial \bar{t}} = \frac{1}{P_r}\frac{\partial^2 \theta}{\partial R^2} + \frac{1}{RP_r}\frac{\partial \theta}{\partial R} \tag{7}$$

$$\frac{\partial \bar{C}}{\partial \bar{t}} = \frac{1}{S_c}\frac{\partial^2 \bar{C}}{\partial R^2} + \frac{1}{RS_c}\frac{\partial \bar{C}}{\partial R} - K_0\bar{C} \tag{8}$$

$$\begin{aligned} &\bar{u}(R,0) = 0, \quad \theta(R,0) = 0, \quad C(R,0) = 0, \quad R \in [0,1], \\ &\bar{u}(1,\bar{t}) = \bar{u}_s, \quad \theta(1,\bar{t}) = 1, \quad \bar{C}(1,\bar{t}) = 1; \quad \bar{t} > 0 \\ &\tfrac{\partial \bar{u}(0,\bar{t})}{\partial R} = 0, \quad \tfrac{\theta(0,\bar{t})}{\partial R} = 0, \quad \tfrac{\partial \bar{C}(0,\bar{t})}{\partial R} = 0; \quad \bar{t} > 0 \end{aligned} \tag{9}$$

For simplification, removing bars in the model, we get

$$\frac{\partial u}{\partial t} = \left(1+\frac{1}{\gamma}\right)\frac{\partial^2 u}{\partial R^2} + \frac{1}{R}\left(1+\frac{1}{\gamma}\right)\frac{\partial u}{\partial R} + G_r\theta + G_m C - Mu - \frac{1}{K}u \tag{10}$$

$$\frac{\partial \theta}{\partial t} = \frac{1}{P_r}\frac{\partial^2 \theta}{\partial R^2} + \frac{1}{RP_r}\frac{\partial \theta}{\partial R} \tag{11}$$

$$\frac{\partial C}{\partial t} = \frac{1}{S_c}\frac{\partial^2 C}{\partial R^2} + \frac{1}{RS_c}\frac{\partial C}{\partial R} - K_0 C \tag{12}$$

The boundary conditions become

$$\begin{aligned} &u(R,0) = 0, \quad \theta(R,0) = 0, \quad C(R,0) = 0, \quad R \in [0,1], \\ &u(1,t) = u_s, \quad \theta(1,t) = 1, \quad C(1,\bar{t}) = 1; \quad t > 0 \\ &\tfrac{\partial u(0,t)}{\partial R} = 0, \quad \tfrac{\theta(0,t)}{\partial R} = 0, \quad \tfrac{\partial C(0,t)}{\partial R} = 0; \quad t > 0 \end{aligned} \tag{13}$$

3. Method of Solution to the Problem

Evaluating the behavior of the flow profile within the slipping cylinder, we have used the application of integrated techniques that include the joint Laplace transform and Hankel transforms. According to the concept of cylindrical domain, the finite Hankel transform gets valuable results, while the Laplace transform is used for initial and boundary value problems. By using combined transformations and their inverses, the analytical results will be obtained.

4. Calculation of Temperature Profile

Taking the Laplace transform with respect to t of the dimensionless energy equation (11), subjected to the initial condition (13), we get

$$s\bar{\theta}(r,s) = \frac{1}{P_r}\frac{\partial^2\bar{\theta}}{\partial R^2} + \frac{1}{RP_r}\frac{\partial\bar{\theta}}{\partial R} \tag{14}$$

$$\bar{\theta}(1,s) = \frac{1}{s} \tag{15}$$

Where $\bar{\theta}(r,s)$ is the Laplace transform of the function $\theta(r,t)$ and s is the transformation variable. Then, applying the finite Hankel transform of zero order to equation (14) and using condition (15), give

$$\bar{\theta}_H(r_n,s) = \left(\frac{1}{s} - \frac{1}{s+\frac{1}{P_r}\cdot r_n^2}\right)\frac{J_1(r_n)}{r_n} \tag{16}$$

where $\bar{\theta}_H(r_n,s) = \int_0^1 r\bar{\theta}(r,s)J_0(rr_n)dr$ is the finite Hankel transform of the function $\bar{\theta}(r_n,s)$ and r_n with $n = 0,1,2,3,\ldots$ are positive roots of $J_0(x) = 0$, where J_0 is the Bessel function of the first kind and zero order. Applying the inverse Laplace transform in equation (16), then

$$\theta_H(r_n,t) = \left[1 - \exp(-\frac{r_n^2 t}{P_r})\right]\frac{J_1(r_n)}{r_n} \tag{17}$$

The inverse finite Hankel transform is applied in equation (17), and we get

$$\theta(r,t) = 1 - 2\sum_{n=1}^{\infty}\frac{1}{r_n}\frac{J_o(rr_n)}{J_1(r_n)}\exp\left(-\frac{r_n^2 t}{P_r}\right) \tag{18}$$

5. Calculation of Concentration Profile

Applying the Laplace transform with respect to t into equation (12), subjected to the initial condition (13), we have

$$s\bar{C}(r,s) = \frac{1}{S_c}\frac{\partial^2\bar{C}}{\partial R^2} + \frac{1}{RS_c}\frac{\partial\bar{C}}{\partial R} - K_0\bar{C} \tag{19}$$

$$\bar{C}(1,s) = \frac{1}{s} \tag{20}$$

where, $\bar{C}(r,s)$ is the Laplace transform of the function $C(r,t)$ and s is the transformation variable. After that, applying the finite Hankel transform of zero order to equation (19) and using condition (20), it gives

$$\bar{C}_H(r_n,s) = \begin{pmatrix} \frac{1}{s} - \frac{1}{\left(s+\frac{1}{S_c}r_n^2+K_0\right)} \\ -\frac{K_0}{s\left(s+\frac{1}{S_c}r_n^2+K_0\right)} \end{pmatrix} \frac{J_1(r_n)}{r_n} \tag{21}$$

where $\bar{C}_H(r_n,s) = \int_0^1 r\bar{C}(r,s)J_0(rr_n)dr$ is the finite Hankel transform of the function $\bar{C}(r_n,s)$ and r_n with $n = 0,1,2,3,\ldots$ are positive roots of $J_0(x) = 0$, where J_0 is the Bessel function of the first kind and zero order. Applying the inverse Laplace transform in equation (21), then

$$C_H(r_n,t) = \left(1 - \exp\left(-\left(\frac{1}{S_c}r_n^2 + K_0\right)t\right) - \frac{K_0\exp\left(-\left(\frac{1}{S_c}r_n^2+K_0\right)t\right)}{\frac{1}{S_c}r_n^2+K_0}\right)\frac{J_1(r_n)}{r_n} \tag{22}$$

By using the inverse finite Hankel transform in equation (22), we get

$$C(r,t) = 1 - 2\sum_{n=1}^{\infty}\frac{J_o(rr_n)}{r_nJ_1(r_n)}\exp\left(-\left(\frac{1}{S_c}r_n^2+K_0\right)t\right) - 2\sum_{n=1}^{\infty}\frac{J_o(rr_n)}{r_nJ_1(r_n)}\frac{K_0\exp\left(-\left(\frac{1}{S_c}r_n^2+K_0\right)t\right)}{\frac{1}{S_c}r_n^2+K_0} \tag{23}$$

6. Calculation of Velocity Profile

Taking the Laplace transform with respect to t into the non-dimensional momentum equation (10), subjected to the initial condition (13), we have

$$s\bar{u}(r,s) = \beta\left(\frac{\partial^2\bar{u}(r,s)}{\partial R^2} + \frac{1}{R}\frac{\partial\bar{u}(r,s)}{\partial R}\right) + G_r\bar{\theta}(r,s) + G_m\bar{C}(r,s) - M\bar{u}(r,s) - \frac{1}{K}\bar{u}(r,s) \tag{24}$$

$$\bar{u}(1,s) = \frac{u_s}{s}, \tag{25}$$

where $\beta = \left(1+\frac{1}{\gamma}\right)$ and $\bar{u}(r,s)$ is the Laplace transform of the function $u(r,t)$ and s is the transformation variable. Again, applying the finite Hankel transform of zero order to equation (24) and using condition (25), gives

$$\bar{u}_H(r_n,s) = F_1(s) + F_2(s) + F_3(s), \tag{26}$$

where

$$F_1(s) = \frac{\beta r_n^2}{s(s+\beta r_n^2+M+\frac{1}{K})}\frac{u_sJ_1(r_n)}{r_n} \tag{27}$$

$$F_2(s) = \frac{G_r}{(s+\beta r_n^2+M+\frac{1}{K})}\bar{\theta}_H(r_n,s) \tag{28}$$

$$F_3(s) = \frac{G_m}{(s+\beta r_n^2+M+\frac{1}{K})}\bar{C}_H(r_n,s) \tag{29}$$

where $\bar{u}_H(r_n,s)=\int_0^1 r\bar{u}(r,s)J_0(rr_n)dr$ is the finite Hankel transform of the function $\bar{u}(r_n,s)$ and r_n with $n=0,1,2,3,\ldots$ are positive roots of $J_0(x)=0$, where J_0 is the Bessel function of the first kind and zero order. Applying the inverse Laplace transform to equation (26), then

$$u_H(r_n,t)=f_1(t)+f_2(t)+f_3(t) \tag{30}$$

$$f_1(t)=\left(1-\exp(-(\beta r_n^2+M+\frac{1}{K})t)-\left(M+\frac{1}{K}\right)\frac{1-\exp(-(\beta r_n^2+M+\frac{1}{K})t)}{\beta r_n^2+M+\frac{1}{K}}\right)\frac{u_s J_1(r_n)}{r_n} \tag{31}$$

$$\begin{aligned}f_2(t)&=G_r\frac{J_1(r_n)}{r_n}\frac{1-\exp(-(\beta r_n^2+M+\frac{1}{K})t)}{\beta r_n^2+M+\frac{1}{K}}\\&+G_r\frac{J_1(r_n)}{r_n}\frac{\exp(-(\frac{1}{P_r}\cdot r_n^2))-\exp(-(\beta r_n^2+M+\frac{1}{K}))}{(\frac{1}{P_r}\cdot r_n^2)-(\beta r_n^2+M+\frac{1}{K})}\end{aligned} \tag{32}$$

$$\begin{aligned}f_3(t)&=G_m\frac{J_1(r_n)}{r_n}\frac{1-\exp(-(\beta r_n^2+M+\frac{1}{K})t)}{\beta r_n^2+M+\frac{1}{K}}\\&+G_m\frac{J_1(r_n)}{r_n}\frac{\exp(-(\frac{1}{S_c}r_n^2+K_0)t)-\exp(-(\beta r_n^2+M+\frac{1}{K})t)}{(\frac{1}{S_c}r_n^2+K_0)-(\beta r_n^2+M+\frac{1}{K})}\\&-K_0G_m\frac{J_1(r_n)}{r_n}\frac{1}{(\beta r_n^2+M+\frac{1}{K})(\frac{1}{S_c}r_n^2+K_0)}\\&-K_0G_m\frac{J_1(r_n)}{r_n}\frac{\exp(-(\beta r_n^2+M+\frac{1}{K})t)}{(\beta r_n^2+M+\frac{1}{K})\left((\beta r_n^2+M+\frac{1}{K})-(\frac{1}{S_c}r_n^2+K_0)\right)}\\&-K_0G_m\frac{J_1(r_n)}{r_n}\frac{\exp(-(\frac{1}{S_c}r_n^2+K_0)t)}{\left((\beta r_n^2+M+\frac{1}{K})-(\frac{1}{S_c}r_n^2+K_0)\right)(\frac{1}{S_c}r_n^2+K_0)}\end{aligned} \tag{33}$$

Finally, the inverse finite Hankel transform is applied in equation (30), and we get the required solution as

$$u(r,t)=g_1(t)+g_2(t)+g_3(t), \tag{34}$$

where

$$\begin{aligned}g_1(t)&=u_s-2u_s\sum_{n=1}^{\infty}\frac{J_o(rr_n)}{r_nJ_1(r_n)}\exp(-(\beta r_n^2+M+\frac{1}{K})t)\\&-2u_s\sum_{n=1}^{\infty}\frac{J_o(rr_n)}{r_nJ_1(r_n)}\left(M+\frac{1}{K}\right)\frac{1-\exp(-(\beta r_n^2+M+\frac{1}{K})t)}{\beta r_n^2+M+\frac{1}{K}}\end{aligned} \tag{35}$$

$$\begin{aligned}g_2(t)&=2\sum_{n=1}^{\infty}\frac{J_o(rr_n)}{r_nJ_1(r_n)}G_r\frac{1-\exp(-(\beta r_n^2+M+\frac{1}{K})t)}{\beta r_n^2+M+\frac{1}{K}}\\&+2\sum_{n=1}^{\infty}\frac{J_o(rr_n)}{r_nJ_1(r_n)}G_r\frac{\exp(-(\frac{1}{P_r}\cdot r_n^2)t)-\exp(-(\beta r_n^2+M+\frac{1}{K})t)}{(\frac{1}{P_r}\cdot r_n^2)-(\beta r_n^2+M+\frac{1}{K})}\end{aligned} \tag{36}$$

$$\begin{aligned}g_3(t)&=2\sum_{n=1}^{\infty}\frac{J_o(rr_n)}{r_nJ_1(r_n)}G_m\frac{1-\exp(-(\beta r_n^2+M+\frac{1}{K})t)}{\beta r_n^2+M+\frac{1}{K}}\\&+2\sum_{n=1}^{\infty}\frac{J_o(rr_n)}{r_nJ_1(r_n)}G_m\frac{\exp(-(\frac{1}{S_c}r_n^2+K_0)t)-\exp(-(\beta r_n^2+M+\frac{1}{K})t)}{(\frac{1}{S_c}r_n^2+K_0)-(\beta r_n^2+M+\frac{1}{K})}\\&-2\sum_{n=1}^{\infty}\frac{J_o(rr_n)}{r_nJ_1(r_n)}G_mK_0\frac{1}{(\beta r_n^2+M+\frac{1}{K})(\frac{1}{S_c}r_n^2+K_0)}\end{aligned}$$

$$-2\sum_{n=1}^{\infty}\frac{J_o(rr_n)}{r_nJ_1(r_n)}G_mK_0\frac{\exp(-(\beta r_n^2+M+\frac{1}{K})t)}{(\beta r_n^2+M+\frac{1}{K})\left((\beta r_n^2+M+\frac{1}{K})-(\frac{1}{S_c}r_n^2+K_0)\right)}$$
$$+2\sum_{n=1}^{\infty}\frac{J_o(rr_n)}{r_nJ_1(r_n)}G_mK_0\frac{\exp(-(\frac{1}{S_c}r_n^2+K_0)t)}{\left((\beta r_n^2+M+\frac{1}{K})-(\frac{1}{S_c}r_n^2+K_0)\right)(\frac{1}{S_c}r_n^2+K_0)} \quad (37)$$

7. Validation of the Present Solution

The fluid flow behavior of the obtained analytical solutions for the fluid velocity, temperature, and concentration profile. A limiting case for the present result, Equation (34), has also been observed in this problem to ensure that the current outcome is accurate by comparing it with the published results done by Khan [11]. The result obtained by Khan (by considering $\omega = 0$)

$$u(r,t) = 1+2G_r\sum_{n=1}^{\infty}\frac{J_o(rr_n)}{r_n^3J_1(r_n)}+2\frac{G_r}{P_r-1}\sum_{n=1}^{\infty}\frac{J_o(rr_n)}{r_n^3J_1(r_n)}\left(exp(-r_n^2t)-P_r\exp(-\frac{1}{P_r}r_n^2t)\right)$$
$$-2\sum_{n=1}^{\infty}\frac{J_o(rr_n)}{r_nJ_1(r_n)}\exp(-r_n^2t) \quad (38)$$

In this present study, from our solution (34), (consider $u_s = 1$, $\beta = 1$, $M+\frac{1}{K} = 0$ in equation (34)), then we get

$$u(r,t) = 1-2\sum_{n=1}^{\infty}\frac{J_o(rr_n)}{r_nJ_1(r_n)}\exp(-(r_n^2)t)+2\sum_{n=1}^{\infty}\frac{J_o(rr_n)}{r_nJ_1(r_n)}G_r\frac{1-\exp(-(r_n^2)t)}{r_n^2}$$
$$+\frac{2P_r}{1-P_r}G_r\sum_{n=1}^{\infty}\frac{J_o(rr_n)}{r_n^3J_1(r_n)}\left(\exp(-(\frac{1}{P_r}\cdot r_n^2)t)-\exp(-(r_n^2)t)\right)$$

After simplification, the solution obtained is

$$u(r,t) = 1-2\sum_{n=1}^{\infty}\frac{J_o(rr_n)}{r_nJ_1(r_n)}\exp(-(r_n^2)t)+2G_r\sum_{n=1}^{\infty}\frac{J_o(rr_n)}{r_nJ_1(r_n)}$$
$$-\frac{2P_r}{1-P_r}G_r\sum_{n=1}^{\infty}\frac{J_o(rr_n)}{r_n^3J_1(r_n)}\left(\exp(-(r_n^2)t)-\exp(-(\frac{1}{P_r}\cdot r_n^2)t)\right) \quad (39)$$

So, our solution (39) is the same as the result (38) obtained by Khan [11], and their graphical comparison is shown in Figure 2 and Figure 3, respectively. Hence, the accuracy of the solution to this problem is confirmed.

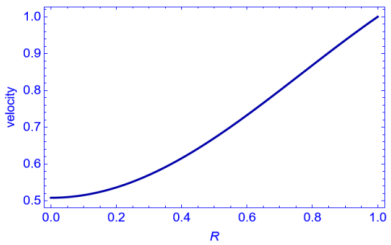

Figure 2

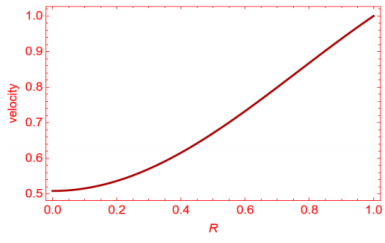

Figure 3

8. Results and Discussion

The motive of the present paper to explain the study of flow behavior of MHD Casson fluid for various parameters like, Casson fluid parameter (γ), chemical reaction (K_o), thermal Grashof number (G_r), mass Grashof number (G_m), permeability parameter (K), magnetic field parameter (M), Prandtl number (P_r), slip and no slip velocity (u_s) and time (t) are shown graphically in Figures 4 to 12. Figure 4 demonstrates a variation of the fluid velocity profile under the impact of slip and no-slip velocity. It is observed that fluid flow velocity near the boundary region increases as the Casson parameter γ rises. The study of the Casson fluid model has a significant role in medical science because the nature of Casson fluid flow behaviour mimics human blood flow via small arteries. The presence of a chemical reaction occurs within the fluid, and then the velocity is decreased (Figure 5). In Figure 6, the velocity profile is present for a variety of mass Grashof numbers. It is clear that the value of velocity rises as the mass Grashof number becomes higher value. Figure 8 illustrates the flow behaviour concerning the Grashof number G_r by having both slip and no-slip effects. According to the graph from Figure 7, the velocity of flow increases as the G_r increases. The Grashof number is significant when dealing with the free convection flow. This is the dimensionless quantity that shows how the buoyancy force and viscosity force acting on a fluid are related. It takes place naturally when there is a change in fluid density due to temperature differences. For example, warm fluid will rise due to the force of buoyancy, while viscous forces resist the buoyancy force. The buoyancy force increases as the Grashof number grows. Figure 8 depicts fluid flow behaviour in the presence of a porous medium with slip and no-slip effects. The porous medium represents the Darcy number. Based on the graph observation, the flow profile slightly rises with the increment of the Darcy number. This is due to the fact that a higher Darcy number causes porous media to have higher permeability. For both cases of slip and no-slip conditions, the velocity of flow decreases as the magnetic parameter M increases. It is presented in Figure 9. The occurrence is caused by the resistive force, also referred to as the Lorentz force, which acts against the flow. The impact of the Prandtl number on flow velocity can be observed in Figure 10. It is clearly explained from Figure 10 that as the Prandtl number P_r increases, velocity decreases for both conditions of slip and no-slip velocity. This is an occurrence because momentum diffusivity and P_r are directly related. Momentum diffusivity increases lead to an increase in the viscous force, which resists the velocity of the fluid. It causes a decrease in fluid velocity in the boundary region. From Figure 11, it is noted that the velocity is decreased about the centre and increases within the boundary region of the surface of the cylinder. The velocity of flow increased with time (Figure 12).

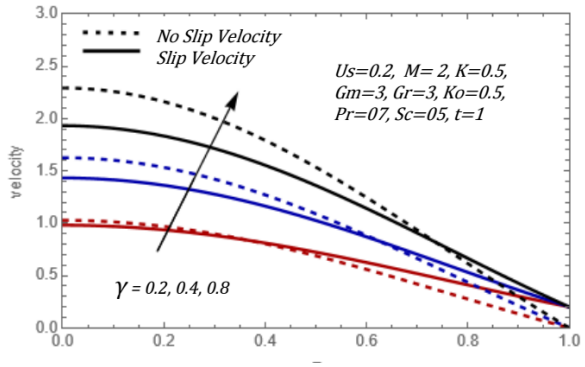

Figure 4: Velocity u for different values of γ

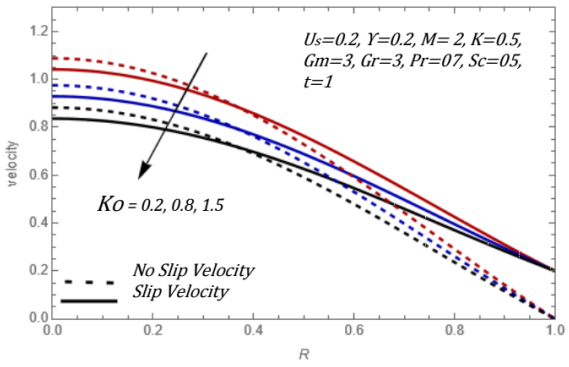

Figure 5: Velocity u for different values of K_o

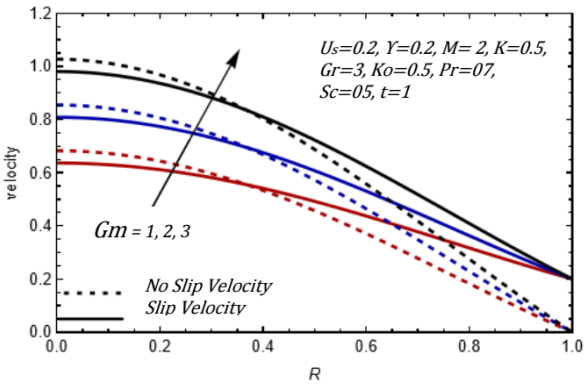

Figure 6: Velocity u for different values of G_m

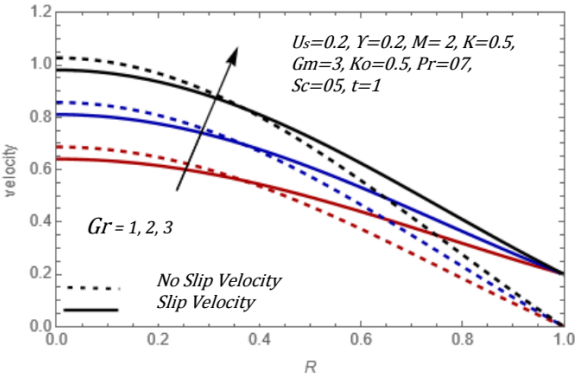

Figure 7: Velocity u for different values of G_r

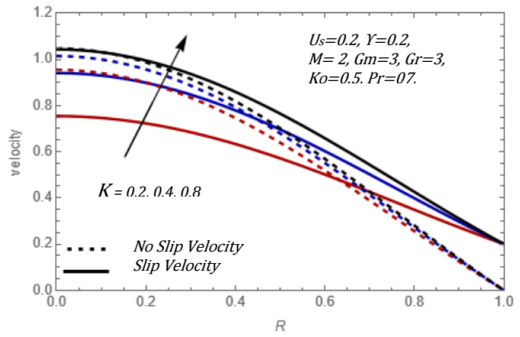

Figure 8: Velocity u for different values of K

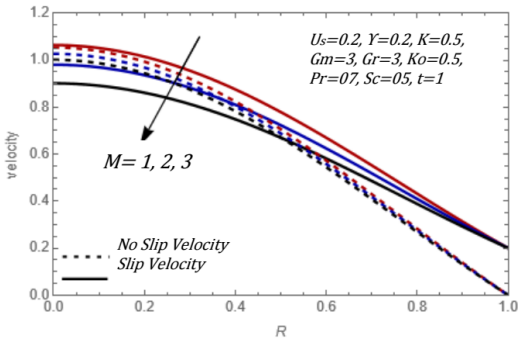

Figure 9: Velocity u for different values of M

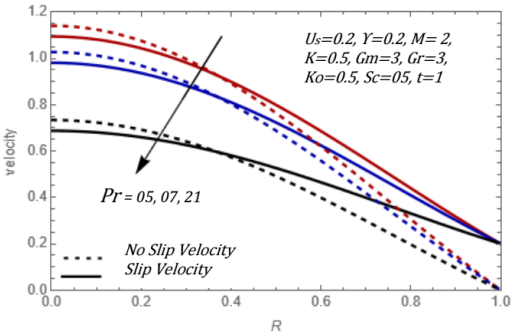

Figure 10: Velocity u for different values of P_r

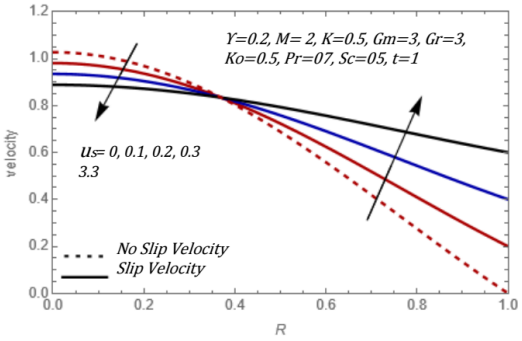

Figure 11: Velocity u for different values of u_s

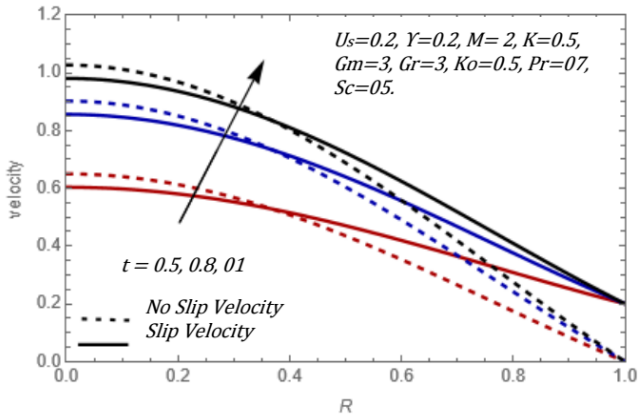

Figure 12: Velocity u for different values of t

9. Conclusion

The analytical solution has been obtained for the slip velocity and chemical reaction effects on unsteady free convection flow of MHD Casson fluid in a cylinder with heat and mass transfer. MHD Casson flow model under the assumption of transforming the governing non-linear equations into dimensionless form. The MHD Casson fluid flow model consists of equations of motion, diffusion, and the energy equation. The governing equations of the non-dimensional form of the flow model have been solved by using the joint Laplace transform and Hankel transform method. To investigate the solutions obtained, standard sets of the values of the parameters have been taken. The results obtained are in agreement with the usual flow. It is observed that the velocity of flow is increased with the Casson parameter, mass, thermal Grashof number, and permeability parameter. However, the velocity profile decreases with chemical reaction, magnetic field parameter, and Prandtl number. The impact of slip velocity is observed as the velocity decreases about the centre and increases within the boundary region of the surface of the cylinder. Thus, these results are beneficial for further exploration in the applications of biomedical engineering and pathology.

References

[1] Yves Nubar, *Blood flow, slip, and viscometry*, Biophysical Journal, 11(3)(1971), 252-264.

[2] T. S. Chen and C. F. Yuh, *Combined heat and mass transfer in natural convection along a vertical cylinder*, Int. J. Heat Mass Transfer, 23(1980), 451-461.

[3] B. Das and R. L. Batra, *Secondary flow of a Casson fluid in a slightly curved tube*, Int. J. Non-Linear Mechanics, 28(5)(1993), 567-577.

[4] R. K. Dash, K. N. Mehta and G. Jayaraman, *Casson fluid flow in a pipe filled with a Homogeneous porous medium*, Int. J. Engng Sci., 34(10)(1996), 1145-1156.

[5] T. Sochi, *Non-Newtonian flow in porous media*, Polymer, 51(2010), 5007-5023.

[6] S. Nadeem, R. U. Haq and C. Lee, *MHD flow of a Casson fluid over an exponentially shrinking sheet*, Scientia Iranica, 19(6)(2012), 1550-1553.

[7] A. Khalid, I. Khan, A. Khan and S. Shafie, *Unsteady MHD free convection flow of Casson fluid past over an oscillating vertical plate embedded in a porous medium*, Eng. Sci. Technol., 18(2015), 309-317.

[8] I. L. Animasaun, E. A. Adebile and A. I. Fagbade, *Casson fluid flow with variable thermo-physical property along exponentially stretching sheet with suction and exponentially decaying internal heat generation using the homotopy analysis method*, Journal of the Nigerian Mathematical Society, 35(2016), 01-17.

[9] M. Abid, J. Tariq and M. Irfan, *Heat transfer analysis of boundary layer flow over hyperbolic stretching cylinder*, Alexandria Engineering Journal, 55(2016), 1333-1339.

[10] A. A. Afify, *The Influence of Slip Boundary Condition on Casson Nanofluid Flow over a Stretching Sheet in the Presence of Viscous Dissipation and Chemical Reaction*, Math. Probl. Eng., 18(2017), 1-12.

[11] I. Khan, A. Shah, A. Tassaddiq, N. Mustapha and Kechil, *Natural convection heat transfer in an oscillating vertical cylinder*, Plos One, 13(1)(2018).

[12] W. F. Azmi, A. Q. Wan, L. Y. Mohamad and S. S. Jiann, *Analytical solution of unsteady Casson fluid flow through a vertical cylinder with slip velocity effect*. Journal of Advanced Research in Fluid Mechanics and Thermal Sciences, 87(1)(2021), 68-75.

[13] G. Kumar and S. M. K. Rizvi, *Casson fluid flow past a vertical cylinder in the presence of chemical reaction and magnetic field*, Applications and Applied Mathematics: An International Journal (AAM), 16(1)(2021), 524-537.

[14] M. Kumar, G. Kumar and A. W. Khan, *Unsteady MHD flow through porous medium past an exponentially accelerated inclined cylinder with variable oscillating wall temperature in the presence of chemical reaction*, GANITA, 72(2)(2022), 103-113.

[15] A. W. F. Wan, M. A. Qushairi, J. L. Yeou and S. Sharidan, *Slip velocity effect on unsteady free convection flow of Casson fluid in a vertical cylinder*, CFD Letters, 15(5)(2023), 29-41.